GEOSYNTHETIC REINFORCED AND PILE SUPPORTED EMBANKMENTS UNDER STATIC AND CYCLIC LOADING

Claas Heitz[1], Jan Lüking[2] & Hans-Georg Kempfert[3]

[1] *Ed. Zueblin AG. (e-mail: claas.heitz@zueblin.de)*
[2] *University of Kassel. (e-mail: J.Lueking@uni-kassel.de)*
[3] *University of Kassel. (e-mail: geotech@uni-kassel.de)*

Abstract: The paper focuses on the soil improvement system "geosynthetic reinforced and pile supported embankment" (GPE-construction). While the system behaviour under static loading is well-known (soil arching and bearing effect in geosynthetic reinforcement), the bearing behaviour under cyclic loading is not yet fully understood and cannot be predicted. Furthermore, the effect of a pile configuration on the mechanical behaviour of the load transfer from geogrids to piles has not yet been fully investigated.

For the purpose of understanding the issues relating to cyclic loading and GPE, large scale model tests on GPE were carried out to examine the stress distribution in the soil above the pile-heads and the effect of the geosynthetic reinforcement on bearing capacity. Different pile configurations (rectangular and triangular grid system) under static and cyclic loading have been investigated. The investigations were supplemented with numerical and analytical calculations.

Based on the results of the model tests, the main parameters that cause a reduction of the arching effect in soil under cyclic loading have been identified. Critical geometrical and cyclic loading limits were established. For values beyond these limits, a modified calculation procedure is proposed which takes into account a soil arching reduction factor and an increase of the geosynthetic strains. The paper gives a brief overview of the test results and describes the load transfer in geosynthetic reinforced and pile supported embankments under static and cyclic loading.

Keywords: biaxial geogrids, cyclic load, dynamic loads, geogrid, geogrid reinforcement

INTRODUCTION

Static and cyclic loads can be transferred through soft soils deeper strata by geosynthetic-reinforced and pile supported embankments (GPE-construction). This construction method has been used successfully since the beginning of the 1990^{s} (Kempfert *et al.* 1995). The main application of this construction method is for highway and railroad embankments in areas with soft subsoils. Many scientific studies have focused on this subject in recent years and different models have been developed. An overview is given in Heitz (2006).

The basic principle of the soil improvement system relies on an arching effect in the embankment (Figure 1). A load-transfer mechanism is based on the fact that the pile-like elements of the GPE system carry a larger portion of the total loads (forces). The remaining portion of the loads (forces) is carried by the geogrid-layer, which subsequently transfers the load to the piles, by which the load on the soft layer is reduced. As the geogrid sags under loading, the soft layer would react with a supportive reaction pressure.

This current approach is given in detail by *Empfehlungen für Bewehrungen aus Geokunststoffen* (EBGEO, 2008), which led to the development of an arching model by Zaeske (2001) and Zaeske *et al.* (2002). Nevertheless, more research is still necessary on a number of factors. These are the load transfer in the geogrid and the different arching effects in various pile arrangements. Furthermore, the influence of cyclic dynamic loading to the arching system is unknown.

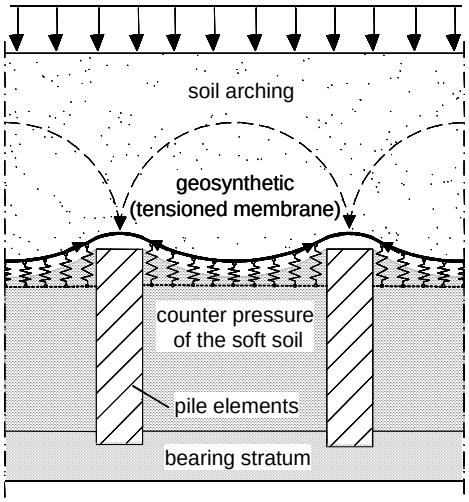

Figure 1. Load transfer mechanism of a GPE-system (after Zaeske 2001)

NUMERICAL CALCULATIONS OF THE LOAD BEARING OF A GPE-CONSTRUCTION IN DIFFERENT GRID ARRANGEMENTS

General

Experience gained in the last few years by the design of GPE-constructions shows that the calculation results after EBGEO (2008) lead to an over design of the geogrid in a triangular grid system. The reason is suspected to be due to an over estimate of the transfer of the bearing load to the piles and the arching effect in soil in a triangular grid system in comparison with a rectangular grid system.

The arching effect in a rectangular grid system is well studied by a number of practitioners/engineers/researchers, among which include Zaeske (2001) and Heitz (2006). However, it is not possible to transfer the experience, and apply the technical knowledge, to a geogrid in a triangular grid system (e.g. Lüking *et al.* 2008). The model tests reported in Lüking *et al.* (2008) have been further investigated by numerical calculations and the essential knowledge is shown in the following sections.

The FEM-software RSTAB version 5 was used for the numerical calculations. The geogrid was simulated as a linear-elastic wire bearing structure. The wires were simply supported at the nodes. The vertical earth pressure was simulated as concentrated loads at the nodes of the system. The numerical models of the geogrid in rectangular and triangular grid systems are shown in Figure 2. Heitz (2006) demonstrated the suitability of using a wire bearing structure calculation for assessment of GPE-construction. The purpose of these numerical calculations was to establish the proportion of the vertical earth pressure imposed directly on the geogrid and to further investigate arching in the soil.

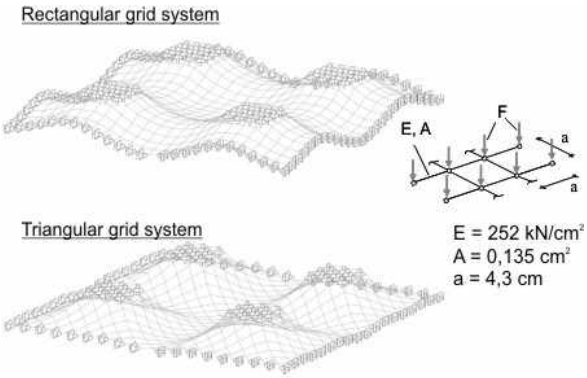

Figure 2. Wire bearing structure for the rectangular and triangular grid system

Geogrid in rectangular grid system

The concentrated loads F (Figure 2) for the numerical calculations were derived from the vertical earth pressure placed directly on the geogrid in the model tests reported by Lüking *et al.* (2008). The vertical earth pressure was converted to the concentrated loads, F, each of which covers an area with dimensions a x a in plan. In areas with no measurements, the concentrated loads were optimised such that the numerical strains calculated were comparable with the measurements of the model tests.

The numerical strains and the results of the model tests reported by Lüking *et al.* (2008) are shown in Figure 3.

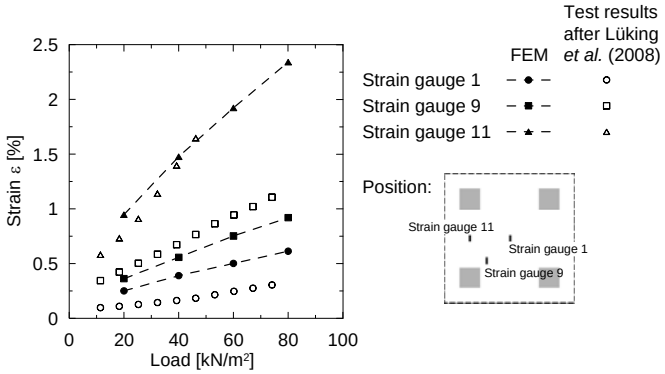

Figure 3. Comparison of strains - numerical calculations and test results after Lüking *et al.* (2008) in a rectangular grid system

The distribution of the vertical earth pressure applied directly on the geogrid could be determined by a back calculation of the concentrated loads over the influenced area. Figure 4 shows the vertical earth pressure in the experimental box at a superimposed load of 60kN/m^2.

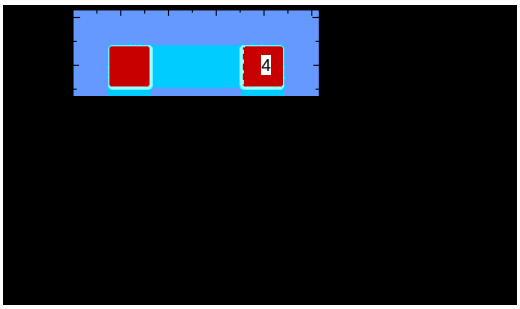

Figure 4. Distribution of the vertical earth pressure directly over the geogrid in rectangular grid systems after the numerical calculations at a surcharge load of 60kN/m^2

A high stress concentration is noticeable over the pile-like elements. On the shortest distance between the pile-like elements a higher stress was calculated in comparison to the middle of the geogrid. The high stress concentration over the pile-like elements results from the bearing of the arching. The higher stress between the shortest distances of the pile-like elements indicates an additional linear bearing of the arching. Because of this, the model of the arching effect in rectangular grid systems shown in Figure 5 (after Heitz 2006) could be confirmed.

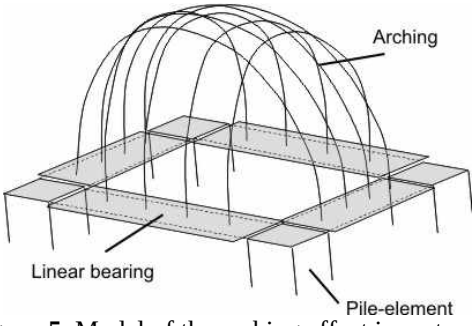

Figure 5. Model of the arching effect in rectangular grid systems after Heitz (2006)

Geogrid in triangular grid system

For numerical calculation of the geogrid in triangular grid systems the concentrated loads F were calibrated to the strains of the geogrid in the rectangular grid system, because in the model tests with geogrids in triangular grid systems no earth pressure sensors were used (Lüking *et al.* 2008). The results are shown in Figure 6.

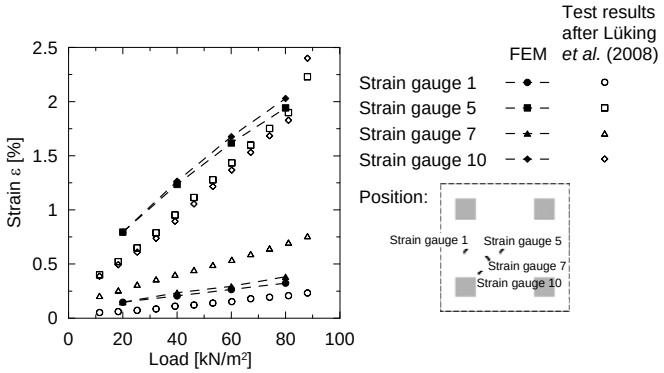

Figure 6. Comparison of strains for the numerical calculations and the test results after Lüking *et al.* (2008) in triangular grid systems

On the basis of these results, the vertical earth pressure distribution directly above the geogrid were determined in a back calculation similar to that used for the rectangular grid system (Figure 7).

The numerical results show that the stress concentration over the pile-like elements is higher than in the rectangular grid system. The stress distribution over the geogrid is more regularly distributed and smaller than in the rectangular grid system. From the calculations, a stress concentration in the middle of the geogrid is clearly visible rather than in the other areas of the geogrid. Because of the different distributions of the vertical earth pressure it is assumed that there is a different arching process in a triangular grid system. The low stress concentration between the shortest distance of the pile-like elements confirms this fact. There is no linear bearing of the arching but rather a spanning in this area. On account of the stress concentration in the middle of the geogrid, it seems that there is a punctual bearing of the arching. The open span of the arching is reduced to allow a more sustainable arching to develop. Also, the higher stress concentration over the pile-like elements is related to this mechanism (i.e. compare Figure 7 with Figure 4). Figure 8 shows the model of the arching effect in triangular grid systems.

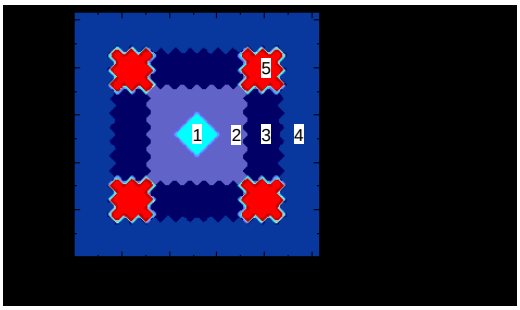

Figure 7. Distribution of the vertical earth pressure directly over the geogrid in triangular grid systems after numerical calculations at a superimposed load of 60kN/m^2

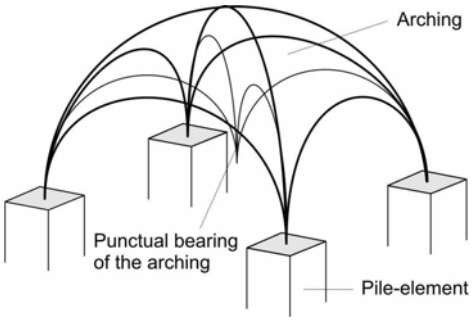

Figure 8. Model of the arching effect in triangular grid systems

GEOSYNTHETIC REINFORCED AND PILE SUPPORTED EMBANKMENT UNDER CYCLIC LOADING

General

Whereas the system behaviour under static loading is well-known (soil arching and bearing effect in geosynthetic reinforcement, see Figure 1) the bearing behaviour under cyclic loading is not yet fully explained and cannot be predicted. For this purpose, large scale model tests were carried out in order to examine the stress-distribution in the soil above the pile-heads and the bearing effect of the geosynthetic reinforcement. The following section gives a short overview of the model tests and the test results, and describes the load transfer in the system under cyclic loading.

Model tests under cyclic loading

The model test arrangement (scale of 1:3) is illustrated in Figure 9. It consists of a group of four piles placed in a weak soil layer (peat) in a rectangular grid and simulates the central zone of a GPE-system. Above the pile heads and the soft soil layer reinforced or unreinforced sand fill of different heights was placed. Pressure cells recorded the stress distribution in the sand fill. Load cells measured the part of the load carried by the piles and this enabled a comparison with the measured stress field in the sand. Strain measurements in the geogrid reinforcement allowed a localisation of the highest tension.

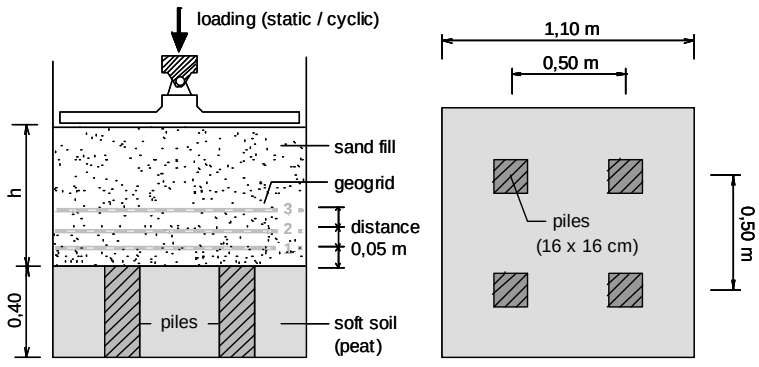

Figure 9. Model test arrangement

Different loading conditions (static and cyclic), different ratios of the height of the sand fill h to the centre-to-centre distance s (h/s = 0,5 / 1,0 / 1,5) and different arrangements of geogrid layers (0 to 3) were investigated. A typical cyclic loading condition (loading frequency f = 1 Hz and 5 Hz; loading amplitude σ_c = +/- 10 kN/m^2; number of load cycles N=1.000.000) is shown in Figure 10.

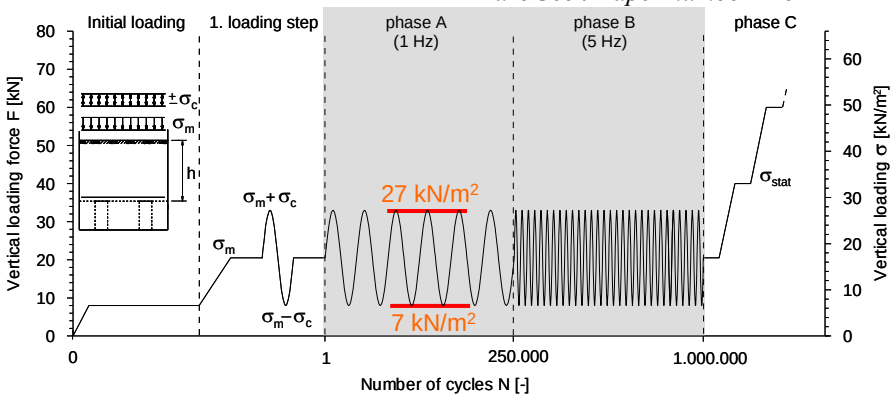

Figure 10. Cyclic loading used in the model tests

The efficiency of soil arching is defined as the efficacy E, which is the ratio of the vertical force F_p on the pile cap to the average force above the pile due to the embankment fill and surcharge load, see equation (1) and Figure 11.

$$E = \frac{F_p}{A_E \cdot (\gamma \cdot h + \sigma)} \qquad (1) \qquad \text{with:} \qquad A_E = s_x \cdot s_y \qquad A_S = b_x \cdot b_y$$

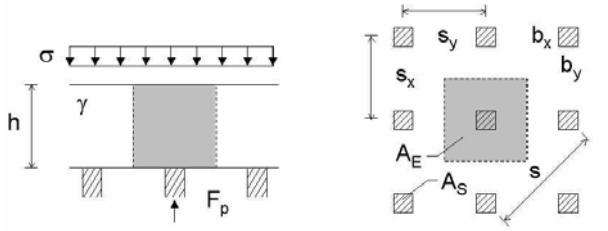

Figure 11. Definition of the efficacy E

Figure 12 shows the measured soil arch ratio in case of h/s = 0,5 and cyclic loading conditions according to Figure 10 for an unreinforced and a reinforced (1 to 3 geogrid layers) system.

Without geosynthetic reinforcement the arching effect can only be formed in a very limited extent under cyclic loading. The part of the load that is carried directly by the piles decrease remarkably during the 1 Hz loading stage from 76 % to 56 %. During the 5 Hz loading stage the soil arch ratio reduces to 39 %. Only a little part of the load is carried directly by the pile-elements and the soil arching effect is nearly nonexistent. Due to the reduction of the soil arching the load on the soft soil and the surface settlements increase considerably. In addition, a punching mechanism of the pile heads through the sand fill takes place, see Heitz (2006) and Heitz *et al.* (2007).

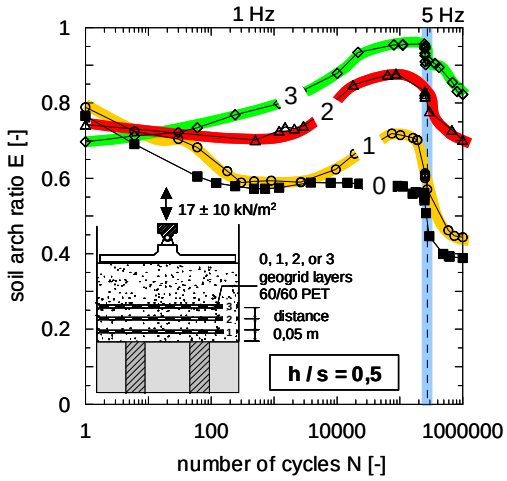

Figure 12. Efficiency of soil arching in case of non- and multi-layered reinforced systems and loading conditions according to Figure 10

The improvement of the soil arching effect by the use of geogrids is also shown in Figure 12. The horizontal geogrid layers stabilise the system under cyclic loading and reduce the settlements of the ground surface. Due to the reduction of the soil arching effect under cyclic loading and the punching mechanism, the strains in the geogrids increase considerably (Figure 13). In particular, the lowest geogrid layers near the pile heads are highly stressed.

The membrane effect in the reinforcement decreases with increasing distance between the pile cap and the geosynthetic layer. The ratio of the maximum strains in the case of two geosynthetic layers is approximately 1:0,66

(strain in lowest layer versus strain in upper layer). For three geosynthetic layers the ratio of the maximum strains is 1:0,66:0,33 (strain in lowest layer versus strain in mid and in upper layer).

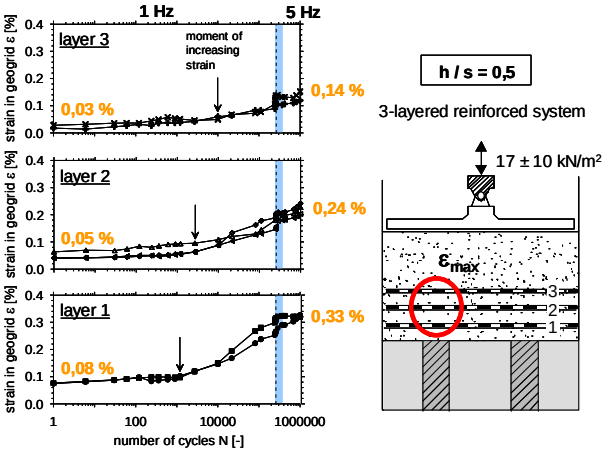

Figure 13. Strains in geosynthetic reinforcement for a three-layered reinforced system and loading conditions according to Figure 10

Based on the results of model tests a factor of soil arching reduction κ was worked out, see equation (2):

$$\kappa = \frac{E_{stat}}{E_{zykl}} \qquad (2)$$

with: E_{stat} soil arch ratio due to static loading
E_{zykl} minimum soil arch ratio during cyclic loading

With the help of the factor κ the main parameters that cause a reduction of the arching effect under cyclic loading can be illustrated, see Figures 14a and 14b. If the loading frequency f, the loading amplitude σ_c and the number of loading cycles N is high, soil arching reduction can take place. In addition, the stability of soil arching is strongly influenced by the ratio h/s (height of the sand fill to the center-to-center distance).

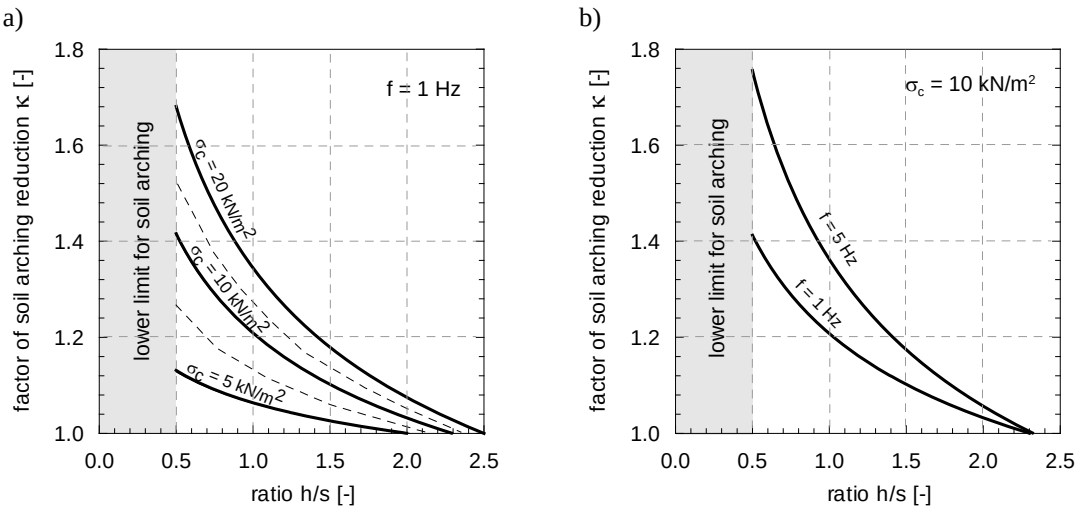

Figure 14. Factor of soil arching reduction κ

Finally, Figure 15 shows the negative effects of cyclic loading on the load transfer mechanisms.

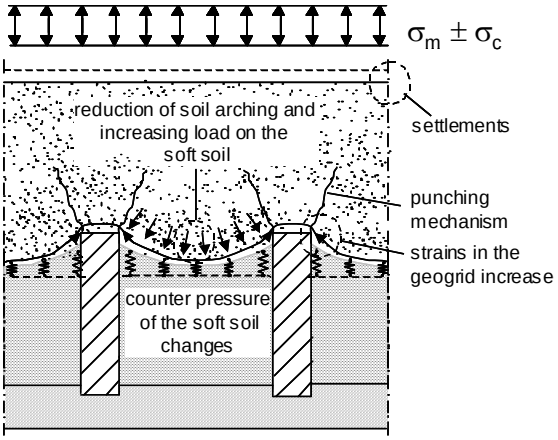

Figure 15. Effects of cyclic lading on the load transfer mechanisms

Analytical calculation of soil arching under static and cyclic loading

For static loading conditions the vertical stress σ_{zo}^{stat} on the soft soil between the piles can be calculated with equation (3) and Figure 16a, see Zaeske (2001) and Kempfert *et al.* (2004).

$$\sigma_{zo}^{stat} = \lambda_1^{-\chi} \cdot \left(\gamma + \frac{\sigma_{stat}}{h}\right) \cdot \left(h \cdot \left(\lambda_1 + h_g^{\,2} \cdot \lambda_2\right)^{-\chi} + h_g \cdot \left(\left(\lambda_1 + \frac{h_g^{\,2} \cdot \lambda_2}{4}\right)^{-\chi} - \left(\lambda_1 + h_g^{\,2} \cdot \lambda_2\right)^{-\chi} \right) \right) \qquad (3)$$

$$\text{with: } h_g = \begin{cases} s/2 & \text{für } h \geq s/2 \\ h & \text{für } h < s/2 \end{cases} \; ; \quad d = 2 \cdot \sqrt{\frac{b_x \cdot b_y}{\pi}}$$

$$K_{krit} = \tan^2\left[45° + \frac{\varphi'}{2}\right] \; ; \; \chi = \frac{d \cdot (K_{krit} - 1)}{\lambda_2 \cdot s} \quad \lambda_1 = \frac{1}{8} \cdot (s - d)^2 \; ; \; \lambda_2 = \frac{s^2 + 2 \cdot d \cdot s - d^2}{2 \cdot s^2}$$

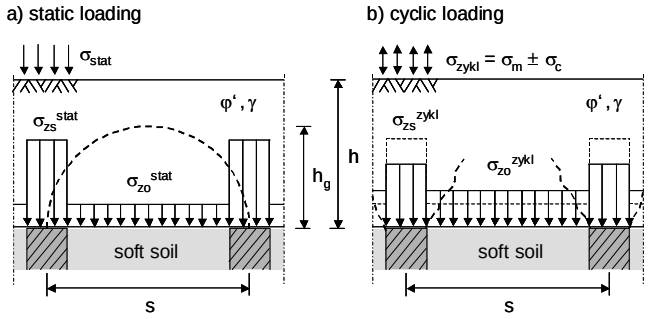

Figure 16. Assumed stresses distribution in case of (a) static or (b) cyclic loading

For cyclic loading conditions a modified calculation procedure is proposed which takes into account a soil arching reduction factor and an increase of the geosynthetic strains. The increased vertical stress σ_{zo}^{zykl} on the soft soil between the piles is calculated with equation (4) and Figure 16b.

$$\sigma_{z0}^{zykl} = \frac{(\gamma \cdot h + \sigma_{stat}) \cdot A_E}{A_E - A_S} \cdot \left(1 - \frac{1}{\kappa}\right) + \frac{1}{\kappa} \cdot \sigma_{z0}^{stat} \qquad (4)$$

As the cyclic loading $\sigma_{zykl}(t)$ is time dependent an equivalent static stress ($\sigma_{stat} = \sigma_m + \sigma_c$) is taken into account within equation (4), see Figure 17. The factor of soil arching reduction κ is taken from Figure 14 depending on the loading frequency f, the loading amplitude σ_c and the ratio h/s.

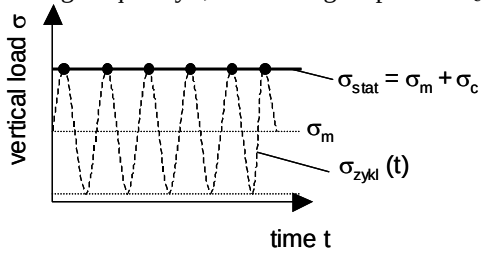

Figure 17. Definition of equivalent static load

Figure 18 illustrates a comparison between the calculated values according to equation (3) and (4) and the model test results. The calculated stresses using equation (4) lie on the safe side.

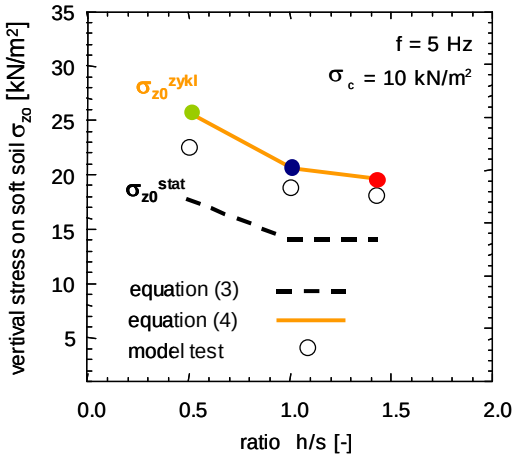

Figure 18. Comparison of equation (3) and (4) and model test results

The additional strains in the geogrids can be calculated using equation (4) and the membrane approach according to Zaeske (2001). Comparison of the analytic and the model test results demonstrates that this design method leads to a conservative prediction of the bearing behaviour of the individual construction elements, see Heitz *et al.* (2007).

SUMMARY

With the help of a point-formed wire-bearing structural model the bearing behaviour of a GPE-construction could be realistically simplified and modelled. The numeric results can confirm the recently derived conceptual model of the arching form for arrangement of geogrid in a rectangular pile grid (Heitz 2006). In addition, for arrangement of geogrid in a triangular pile grid the computations point out that another arching type is formed. Using the numeric results a concepual model could be derived, in which arching is supported by a middle arching-support. Furthermore, with the help of further test series the results can be confirmed.

Cyclic-dynamic loads lead to a changed load-transfer mechanism, as a reformed arching effect in the bearing system takes place. As a result, higher strains in the geogrid and thus a larger load, as well as larger system settlements arise. A soil arching reduction factor could be derived, by which the additional strains in the geogrid due to cyclic-dynamic load can be considered.

REFERENCES

EBGEO 2008. Empfehlungen für Bewehrungen aus Geokunststoffen. Deutsche Gesellschaft für Geotechnik e.V. (DGGT), in preparation

Heitz, C. 2006. Bodengewölbe unter ruhender und nichruhender Belastung bei Berücksichtigung von Bewehrungseinlagen aus Geogittern. Schriftenreihe Geotechnik, University of Kassel, Issue 19

Heitz, C. & Kempfert, H.-G. 2007. Bewehrte Erdkörper über Pfählen unter ruhender und nichtruhender Belastung. Bauingenieur, Issue 9, pp. 380-387

Kempfert, H.-G. & Goebel, C. & Alexiew, D. & Heitz, C. 2004. German Recommendations for Soil Reinforcement above Pile-Elements. EuroGeo 3, 3rd Geosynthetic Conference, Munich, Vol. I, pp. 279-283

Kempfert, H.-G. & Stadel, M. 1995. Zum Tragverhalten geokunststoffbewehrter Erdbauwerke über pfahlähnlichen Traggliedern. Geotechnik Sonderheft zur 4. Informations- und Vortragsveranstaltung über Kunststoffe in der Geotechnik der Deutschen Gesellschaft für Geotechnik e.V. (DGGT), München, pp. 146-152

Lüking, J., Gebreselassie, B., Kempfert, H.-G. 2008. Zum Lastabtrag von Geogittern in geokunststoffbewehrten Erdschichten über Pfahlelementen. 6. Kolloquium „Bauen in Boden und Fels“ der Technischen Akademie Esslingen, Ostfildern, pp. 469-478

Zaeske, D. 2001. Zur Wirkungsweise von unbewehrten und bewehrten mineralischen Tragschichten über pfahlartigen Gründungselementen, Schriftenreihe Geotechnik, University of Kassel, Issue 10

Zaeske, D. & Kempfert, H.-G. 2002. Berechnung und Wirkungsweise von unbewehrten und bewehrten mineralischen Tragschichten über punkt- und linienförmigen Traggliedern. Bauingenieur (77), pp. 80-86